Electronic Supplementary Material (ESI) for Journal of Materials Chemistry A.

SUPPORTING INFORMATION

Two new porous UiO-66-type zirconium frameworks; open aromatic N-donor sites and their post-synthetic methylation and metallation.

Arnold A. Barkhordarian, Cameron J. Kepert

School of Chemistry, The University of Sydney, NSW 2006, Australia.

*Email for correspondence: cameron.kepert@sydney.edu.au

X-ray Diffraction measurements

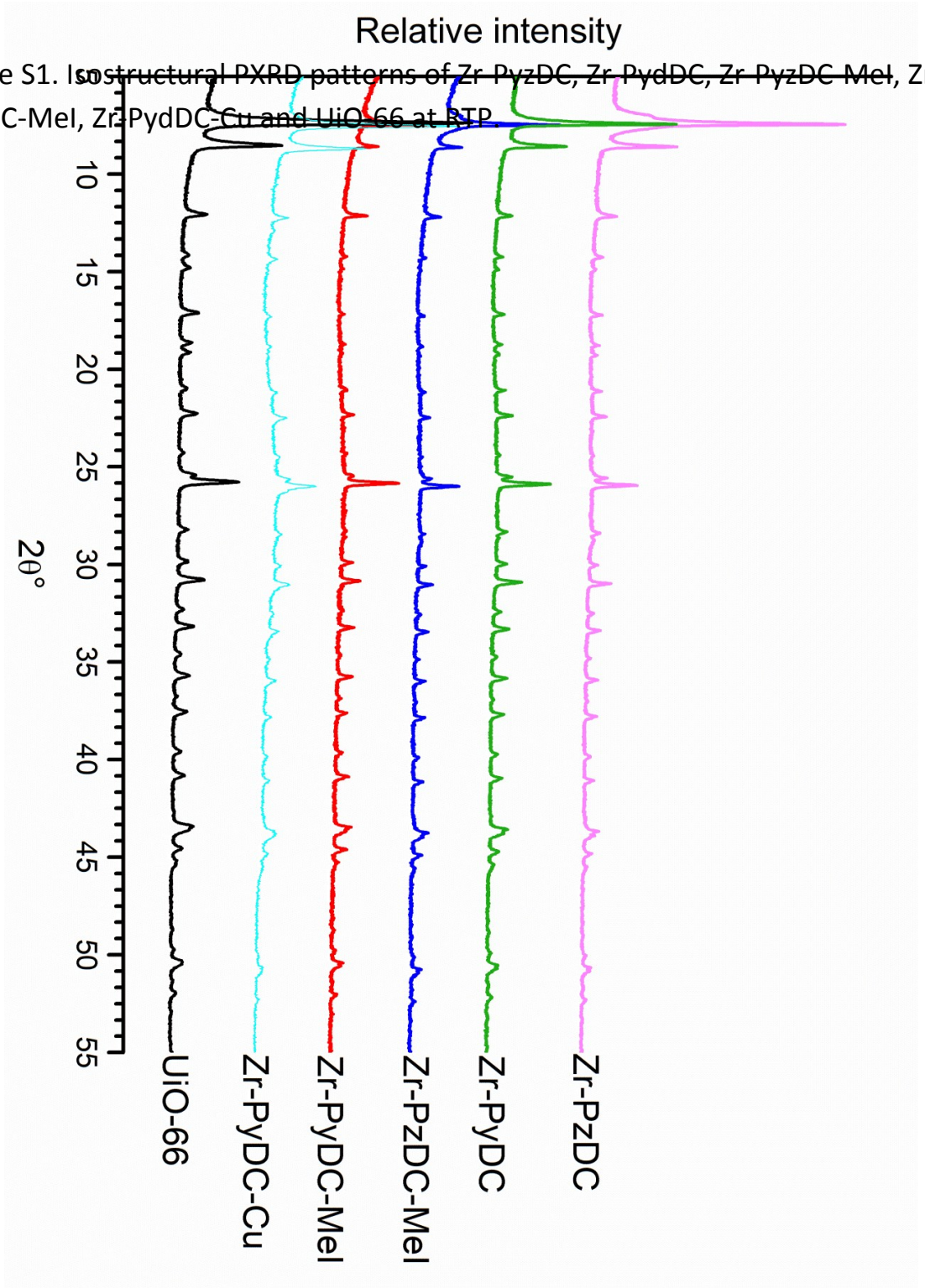

Figure S1. Isostructural PXRD patterns of Zr-PyzDC, Zr-PydDC, Zr-PyzDC-Mel, Zr-PydDC-Mel, Zr-PydDC-Cu and UiO-66 at RTP.

Variable Temperature X-ray Diffraction measurements.

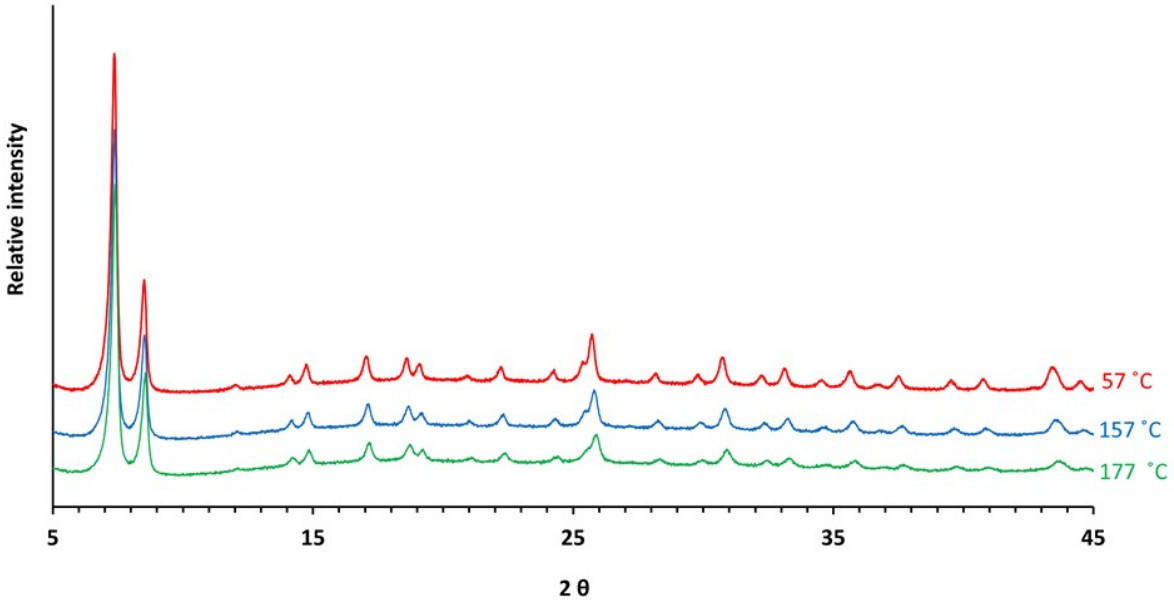

Figure S2. Variable temperature PXRD of UiO-66.

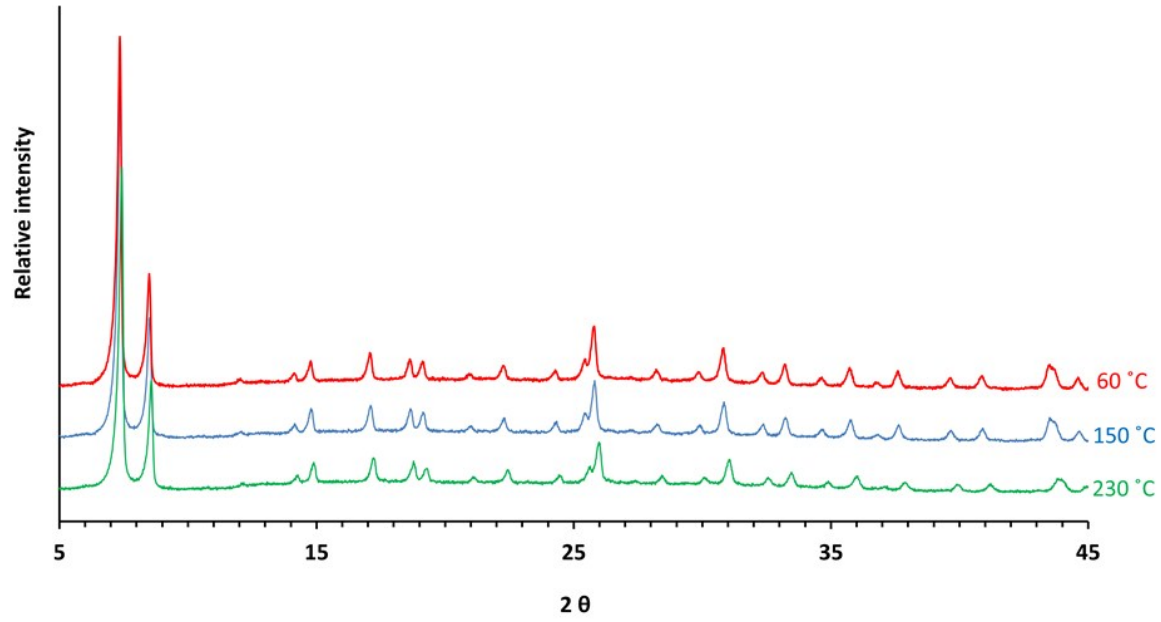

Figure S3. Variable temperature PXRD of Zr-PyDC.

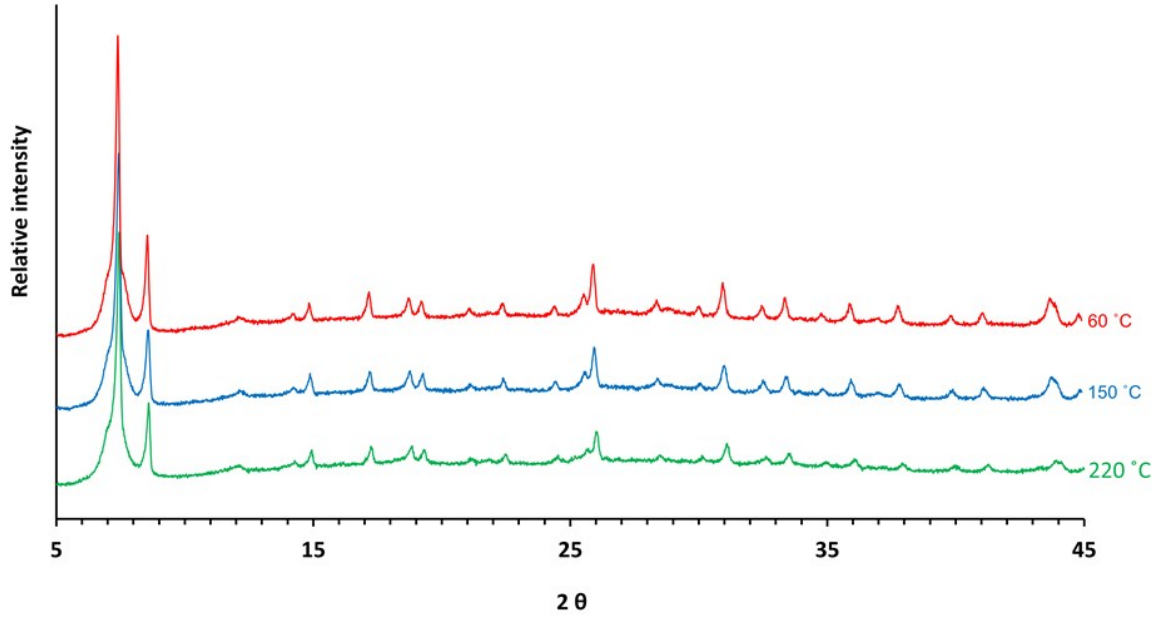

Figure S4. Variable temperature PXRD of Zr-PzDC.

Figure S5. Variable temperature PXRD of Zr-PyDC-MeI.

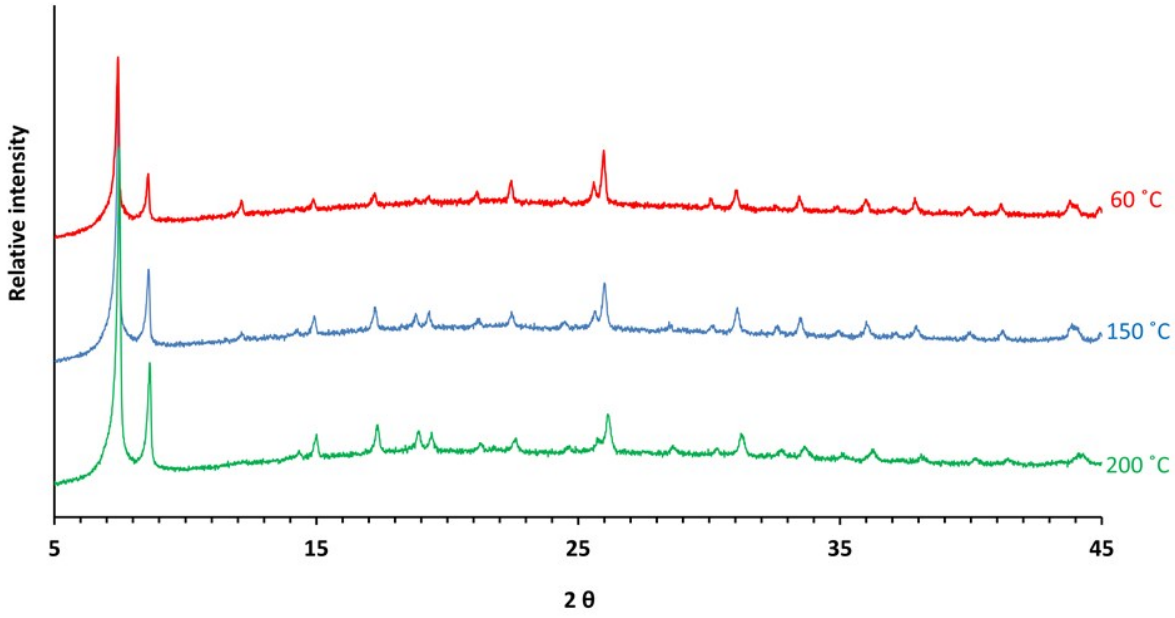

Figure S6. Variable temperature PXRD of Zr-PzDC-MeI.

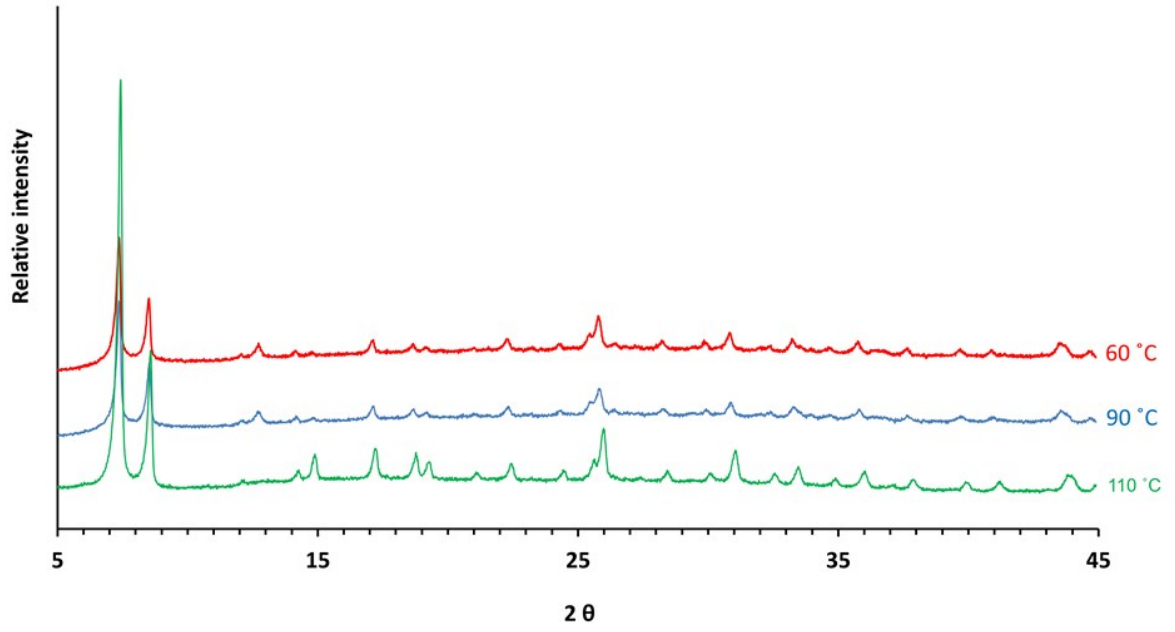

Figure S7. Variable temperature PXRD of Zr-PyDC-Cu.

NMR digest measurements.

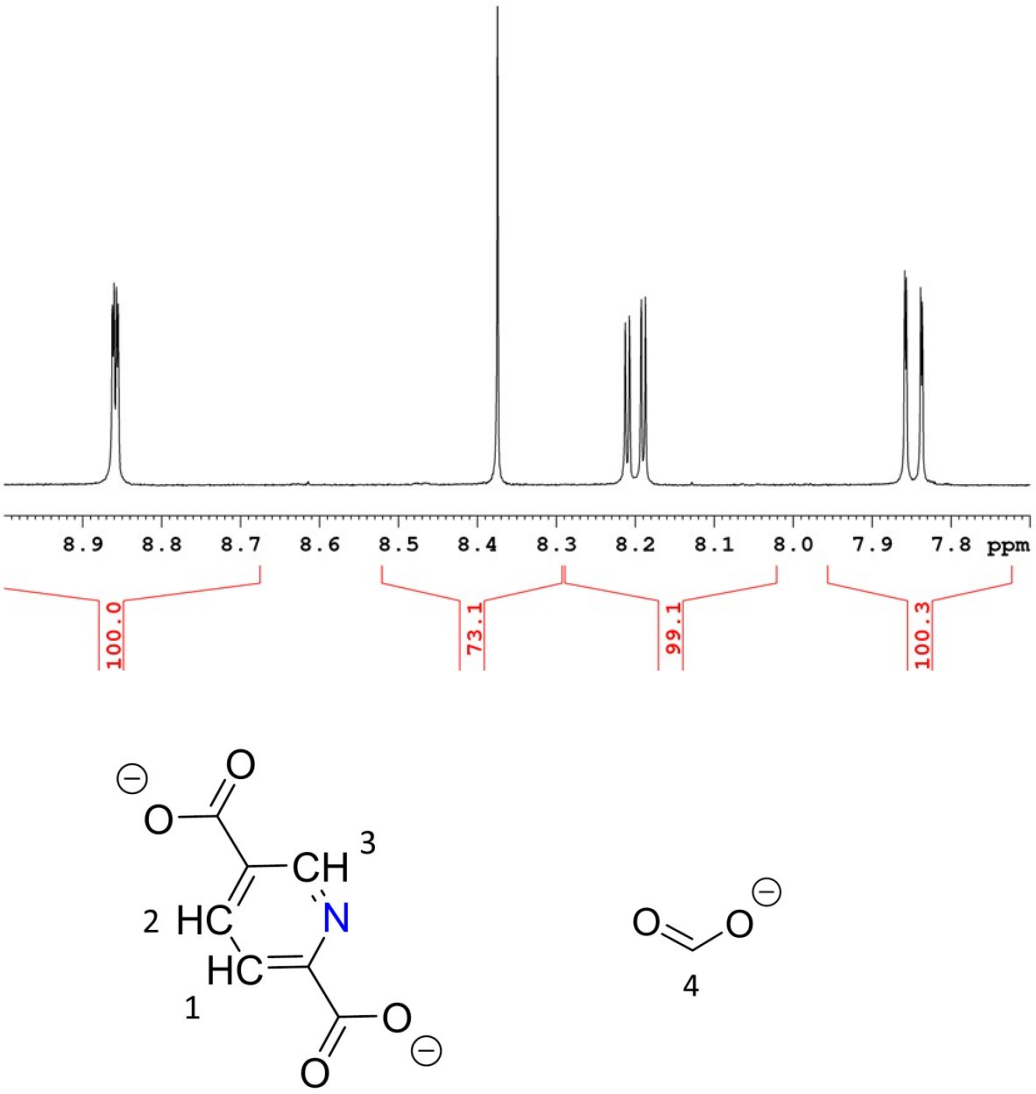

Figure S8. ^{1}H NMR spectra Zr-PyDC. 400MHz, (D_2O KOH) 7.84 (1H, dd, $^{3}J_{H\text{-}H}$ = 8.1 Hz, $^{5}J_{H\text{-}H}$ = 0.9 Hz, H1), 8.20 (1H, dd, $^{3}J_{H\text{-}H}$ = 8.0 Hz, $^{4}J_{H\text{-}H}$ = 2.1 Hz, H2), 8.37 (0.73H, s, H4), 8.86 (1H, dd, $^{4}J_{H\text{-}H}$ = 2.1 Hz, $^{5}J_{H\text{-}H}$ = 0.8 Hz, H3).

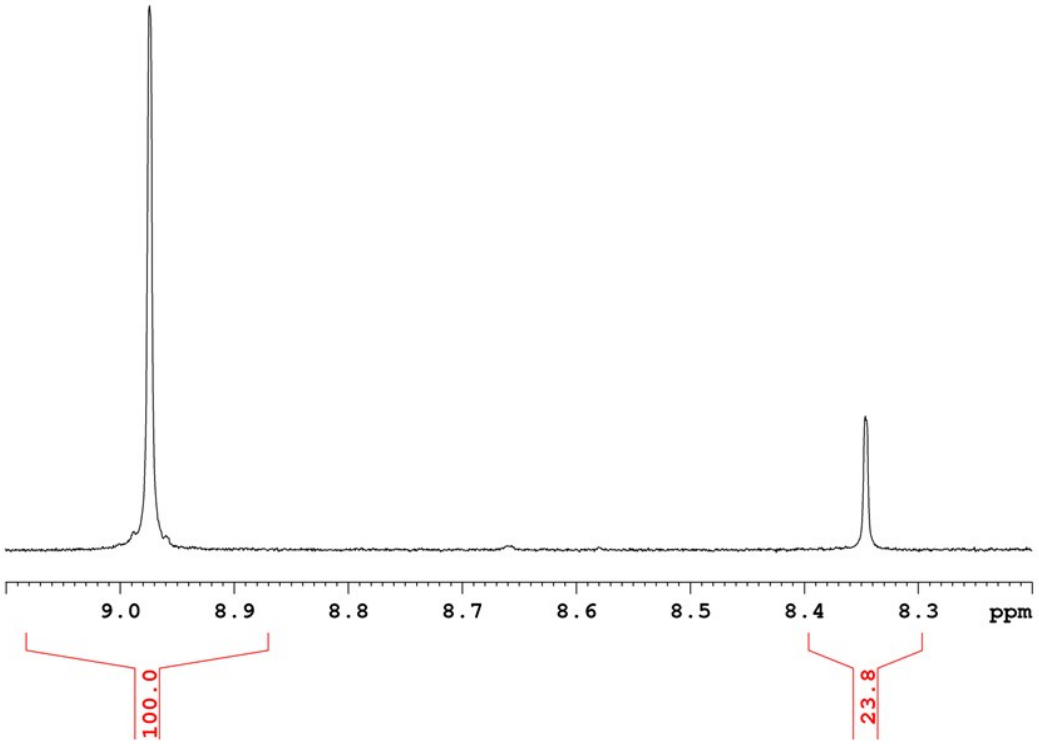

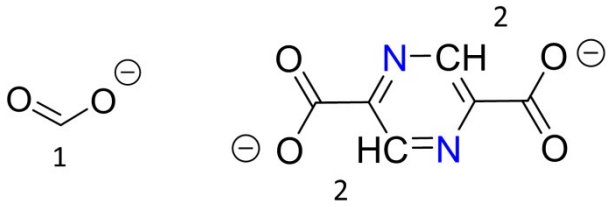

Figure S9. ^{1}H NMR spectra Zr-PzDC. 300MHz, (D_2O KOH) 8.35 (0.24H, s, H1), 8.98 (1H, s, H2).

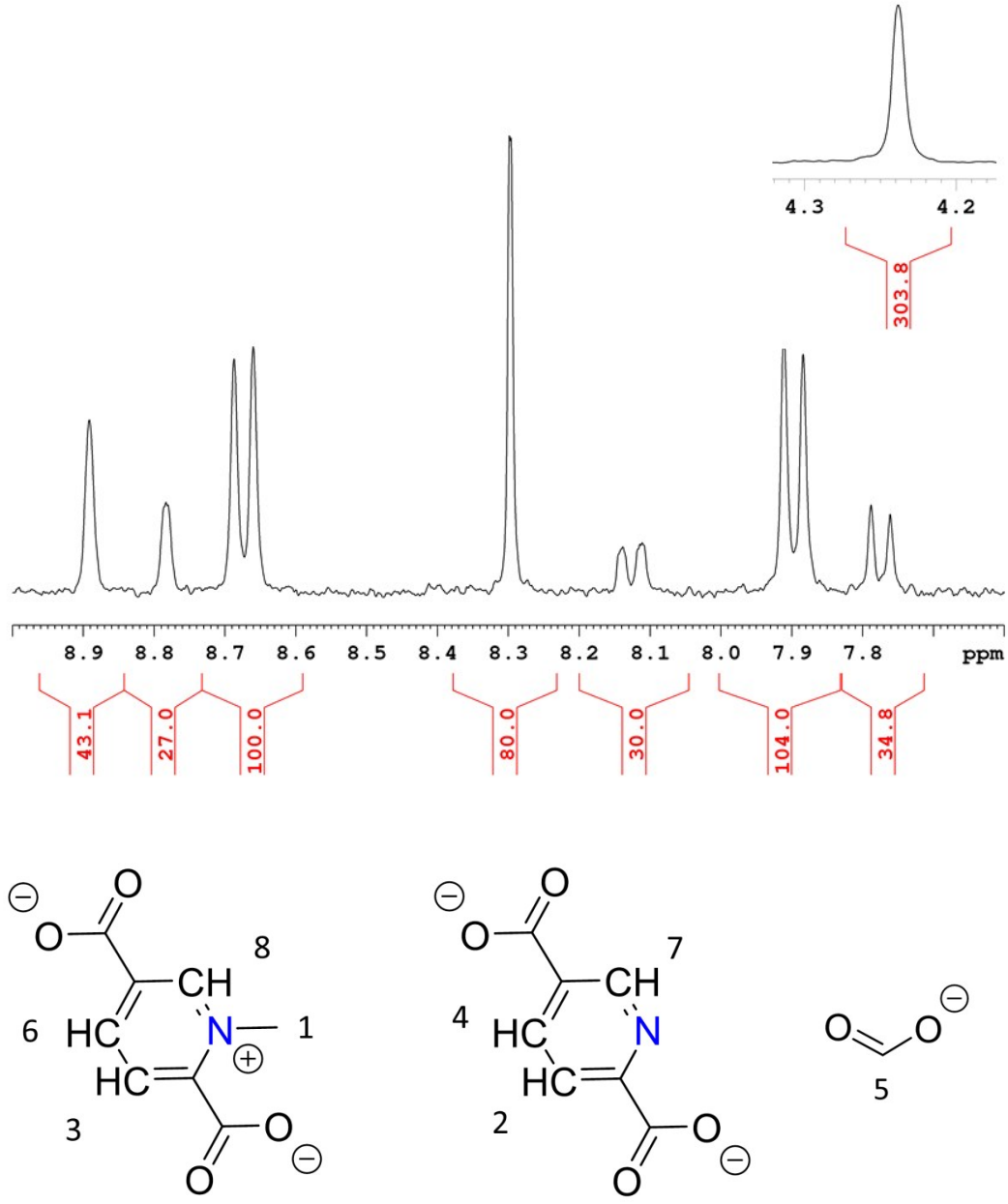

Figure S10. ^{1}H NMR spectra Zr-PyDC-MeI . 300MHz, (D_2O KOH) 4.23 (3H, s, H1), 7.77 (0.3H, d, $^{3}J_{H-H}$ = 8.2 Hz, H2), 7.89 (1H, d, $^{3}J_{H-H}$ = 8.2 Hz, H3), 8.13 (0.3H, d, $^{3}J_{H-H}$ = 8.2 Hz, $^{4}J_{H-H}$ = 2.1 Hz, H4), 8.30 (0.8H, s, H5), 8.67 (1H, d, $^{3}J_{H-H}$ = 8.1 Hz, H6), 8.78 (0.3H, d, $^{4}J_{H-H}$ = 2.1 Hz, H7), 8.89 (0.4H, s, H8).

Note: H8 peak at 8.9 ppm was not used to calculate relative abundance. This proton was underrepresented and the peak observed to diminish with time due to deuterium exchange induced by proximity to N-methyl group.

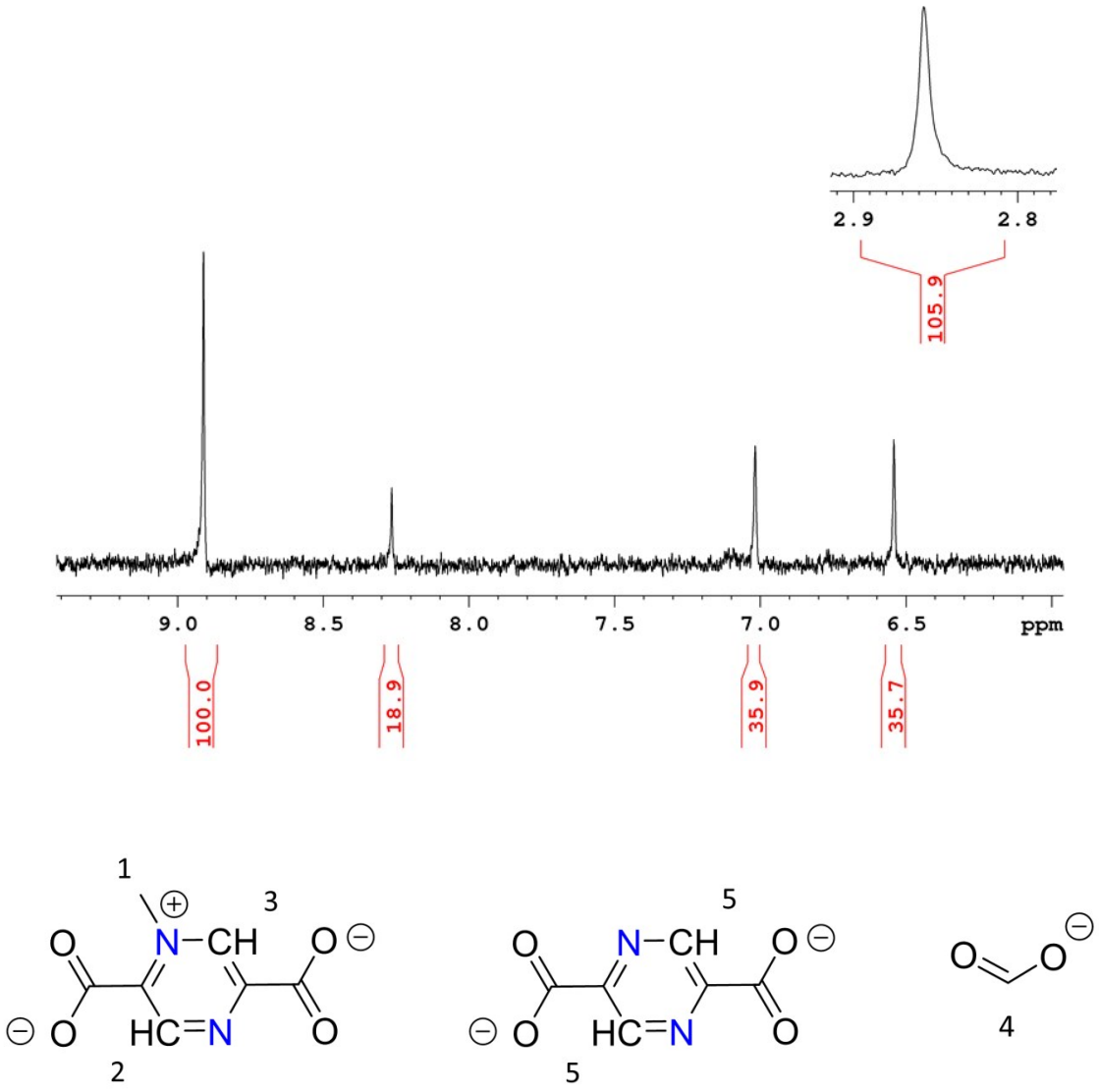

Figure S11. 1H NMR spectra Zr-PzDC-MeI. 300MHz, (D_2O KOH) 2.86 (1H, s, H1), 6.54 (0.36H, s, H2), 7.02 (0.36H, s, H3), 8.27 (0.19H, s, H4), 8.91 (1H, s, H5),

Thermogravimetric analysis

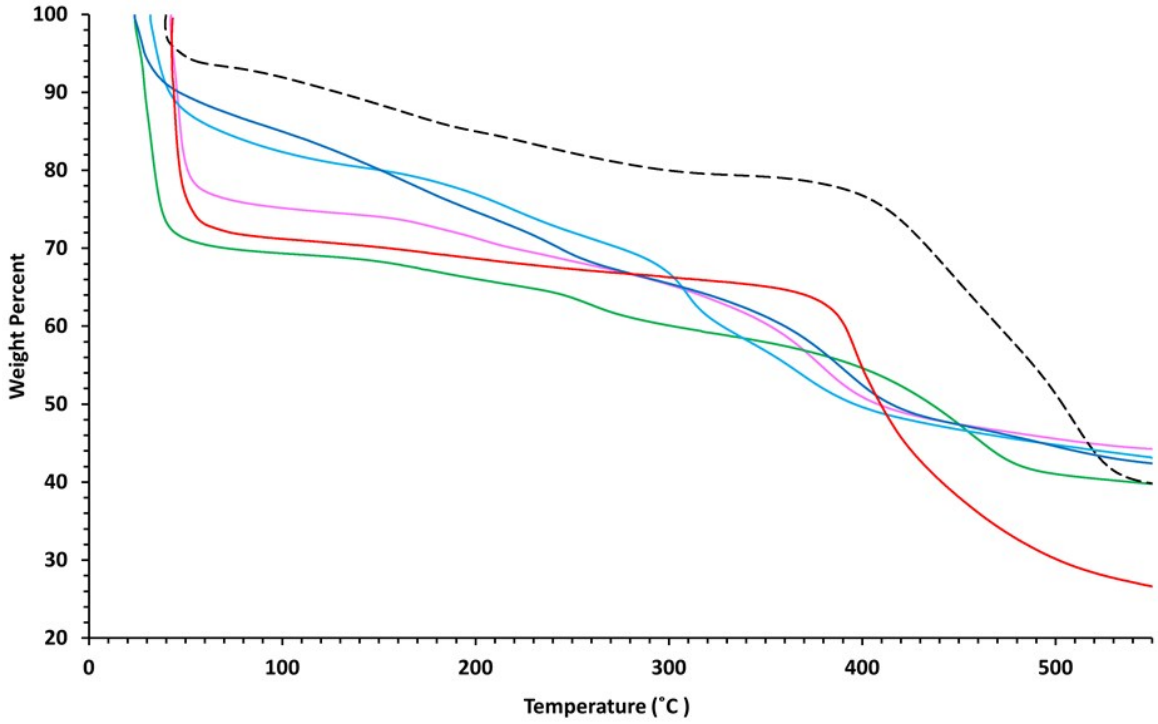

Figure S12. Thermogravimetric analysis of UiO-66 (dashed black), Zr-PyDC (green), Zr-PyDC-MeI (red), Zr-PyDC-Cu (sky blue), Zr-PzDC (pink), Zr-PzDC-MeI (dark blue).

Gas Sorption

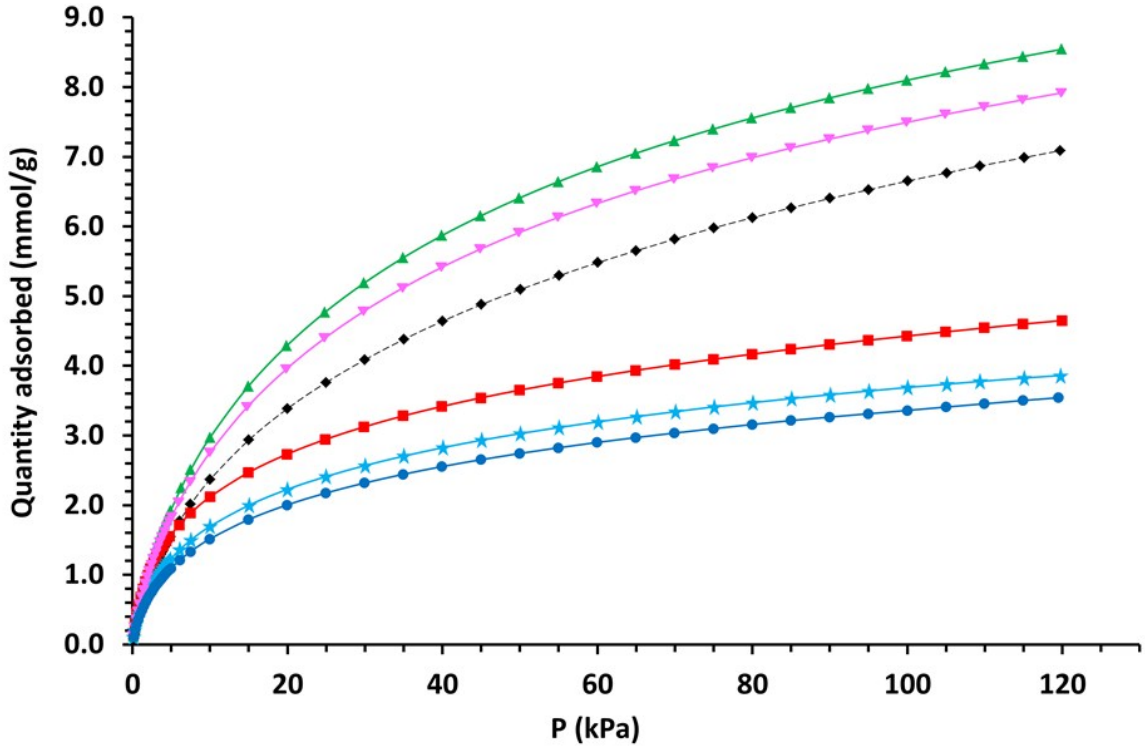

Figure S13. 77K H_2 gas sorption isotherms of UiO-66 (dashed black diamonds), Zr-PyDC (green triangles), Zr-PyDC-MeI (red squares), Zr-PyDC-Cu (sky blue stars), Zr-PzDC (pink inverted triangles), Zr-PzDC-MeI (dark blue circles).

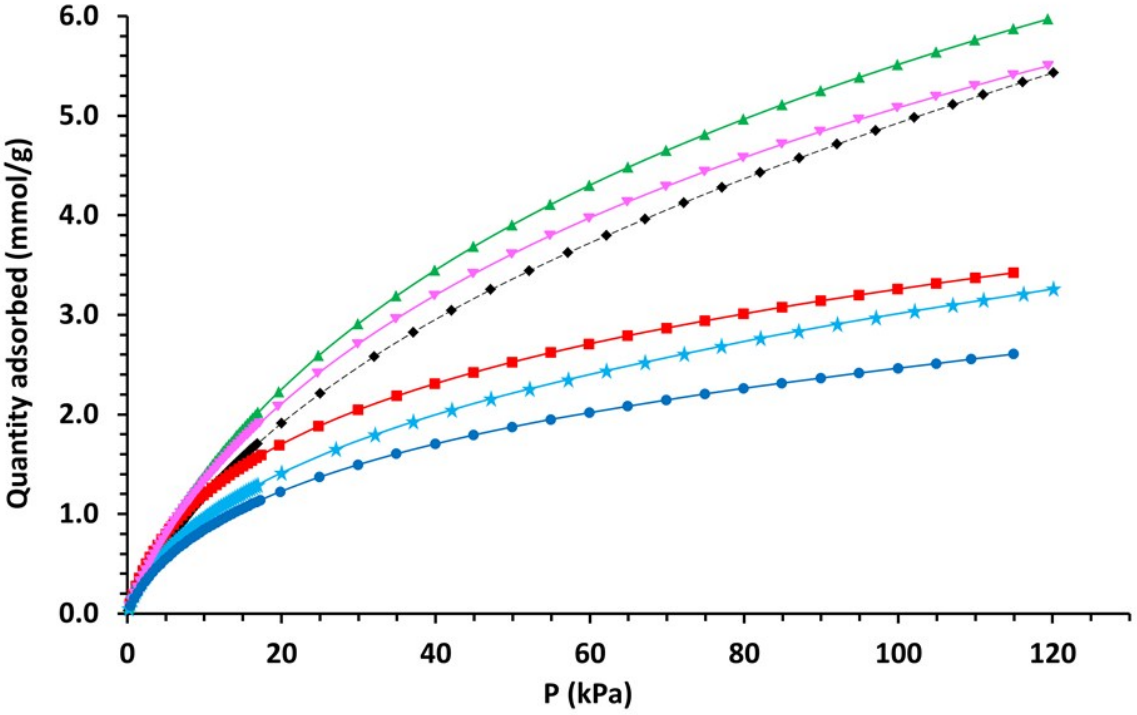

Figure S14. 87K H_2 gas sorption isotherms of UiO-66 (dashed black diamonds), Zr-PyDC (green triangles), Zr-PyDC-MeI (red squares), Zr-PyDC-Cu (sky blue stars), Zr-PzDC (pink inverted triangles), Zr-PzDC-MeI (dark blue circles).

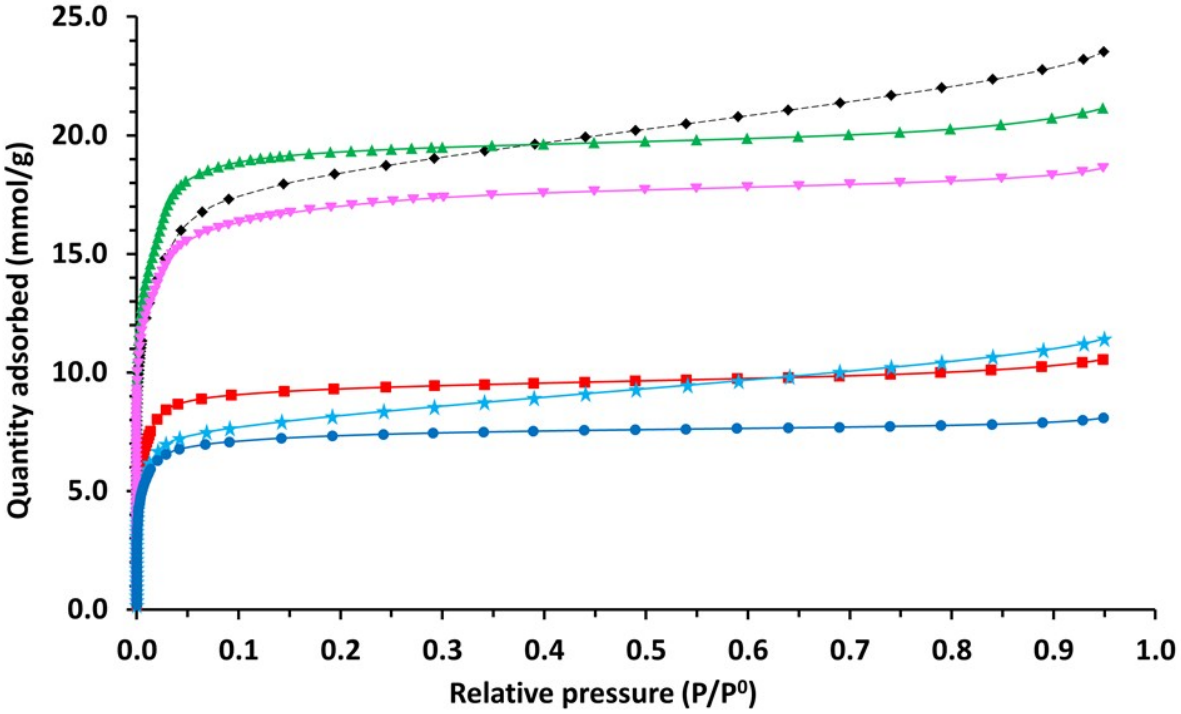

Figure S15. 77K N_2 gas sorption isotherms of UiO-66 (dashed black diamonds), Zr-PyDC (green triangles), Zr-PyDC-MeI (red squares), Zr-PyDC-Cu (sky blue stars), Zr-PzDC (pink inverted triangles), Zr-PzDC-MeI (dark blue circles).

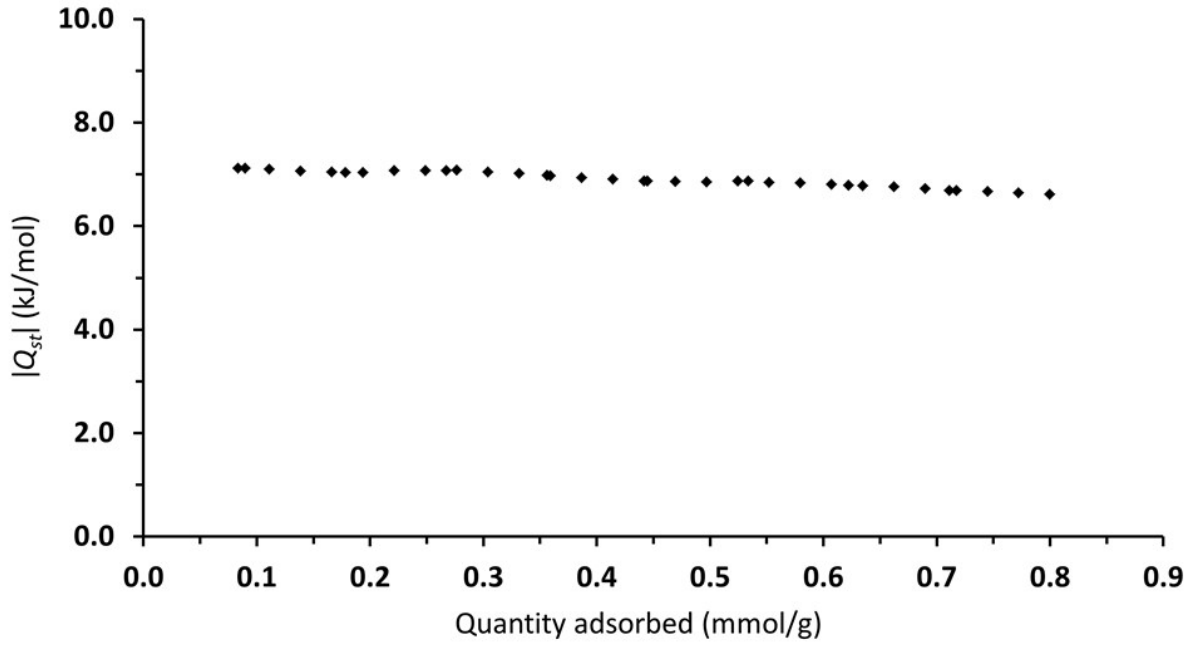

Figure S16. UiO-66 physisorption enthalpy as a function of H_2 loading.

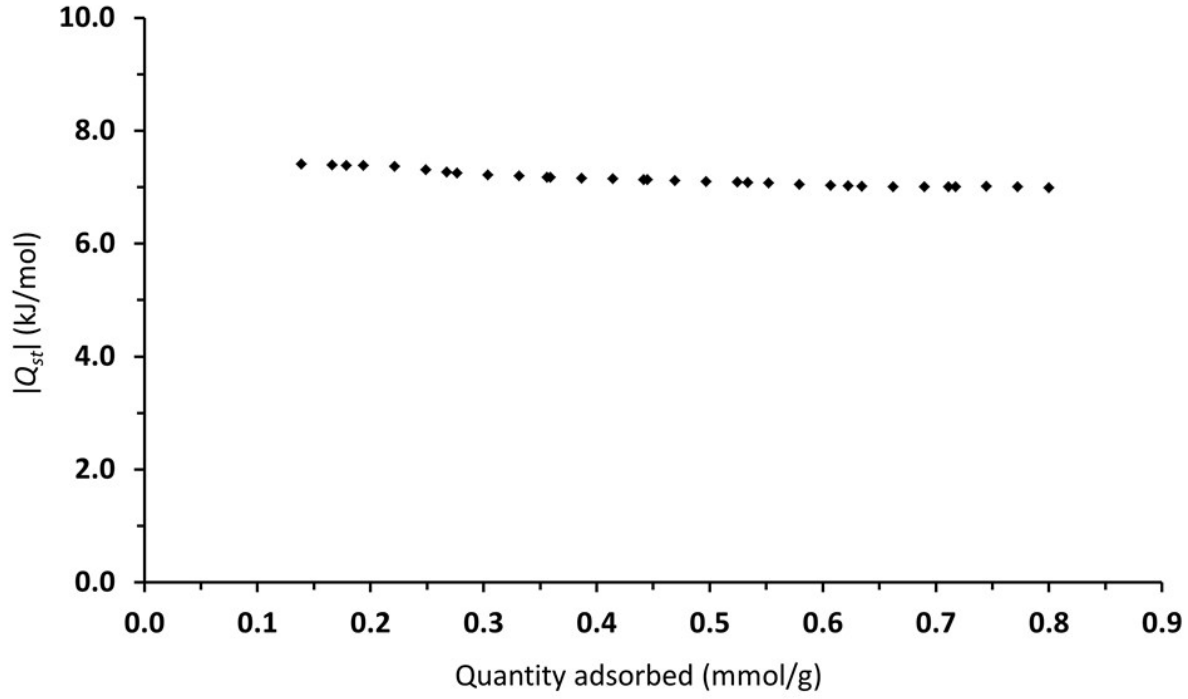

Figure S17. Zr-PyDC physisorption enthalpy as a function of H_2 loading.

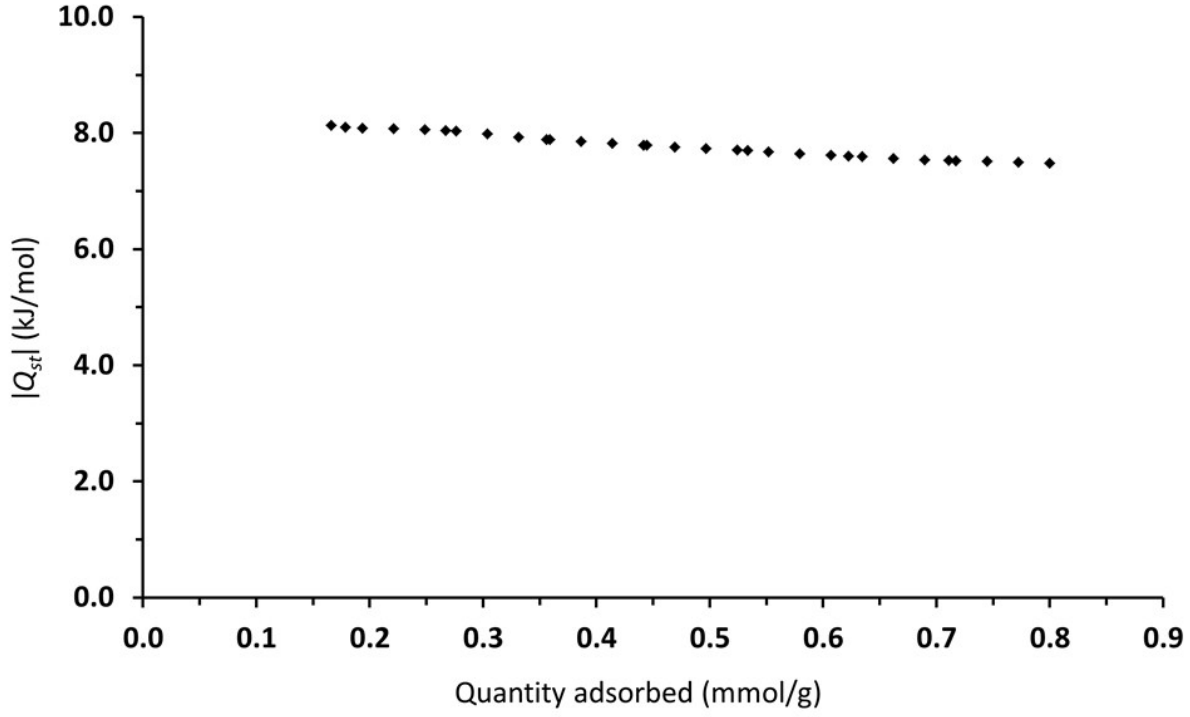

Figure S18. Zr-PyDC-MeI physisorption enthalpy as a function of H_2 loading.

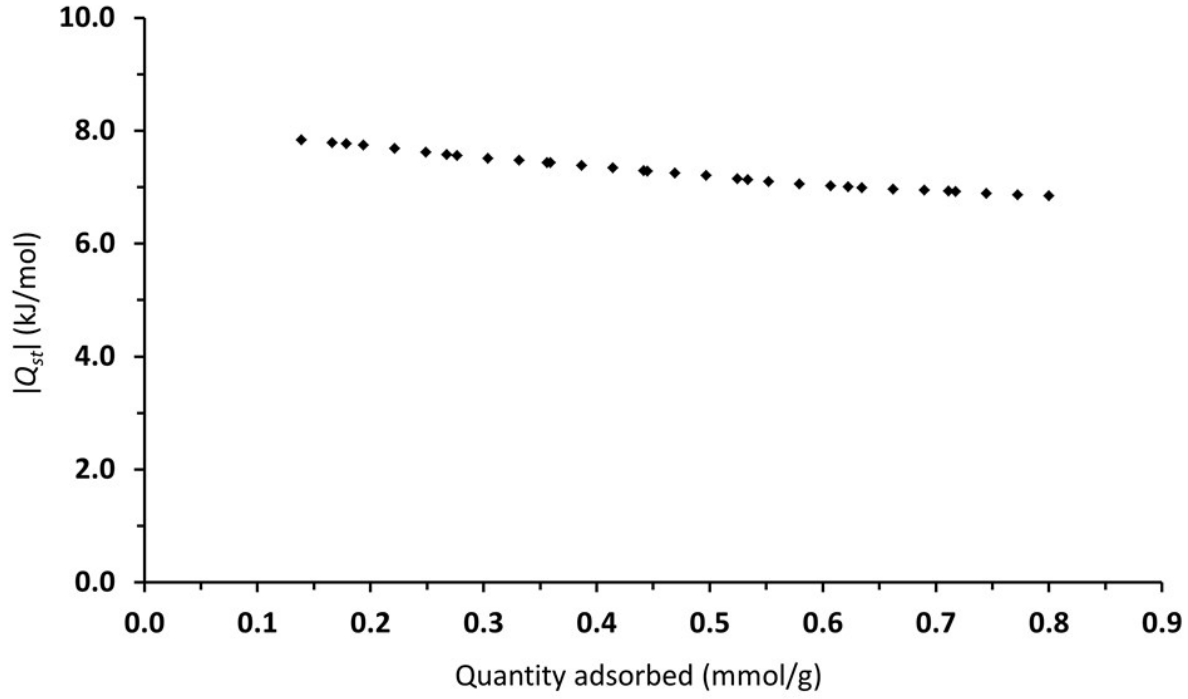

Figure S19. Zr-PzDC-MeI physisorption enthalpy as a function of H_2 loading.

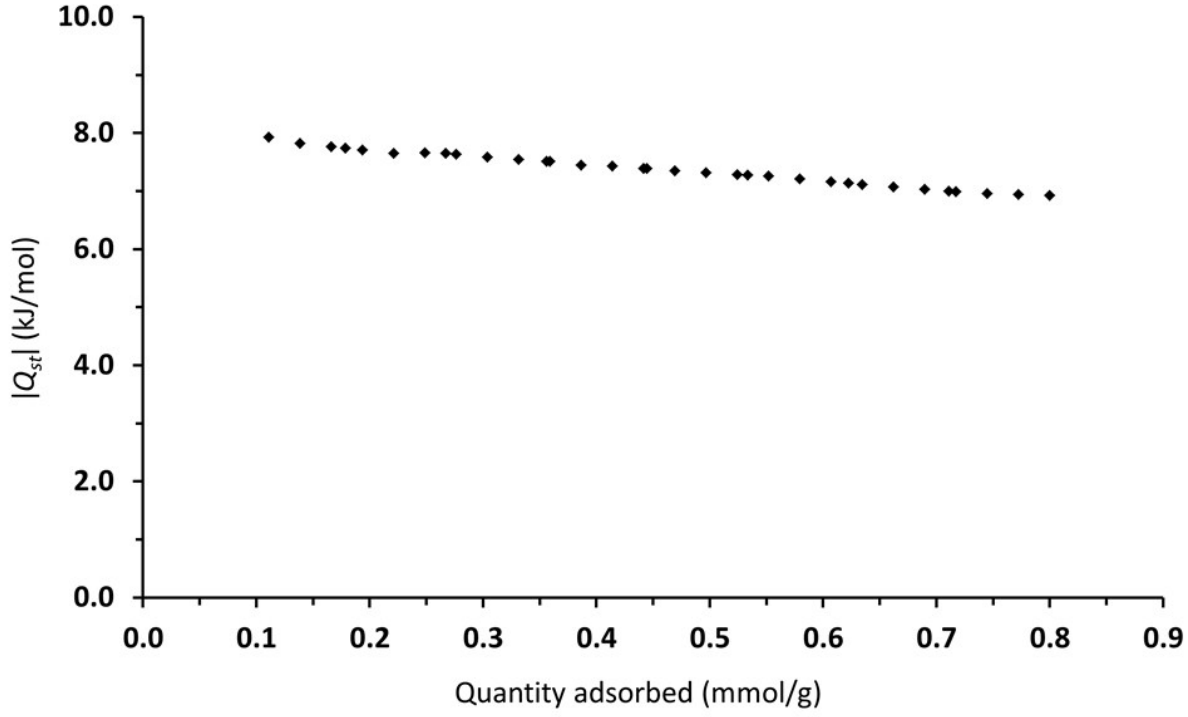

Figure S20. Zr-PyDC-Cu physisorption enthalpy as a function of H_2 loading.

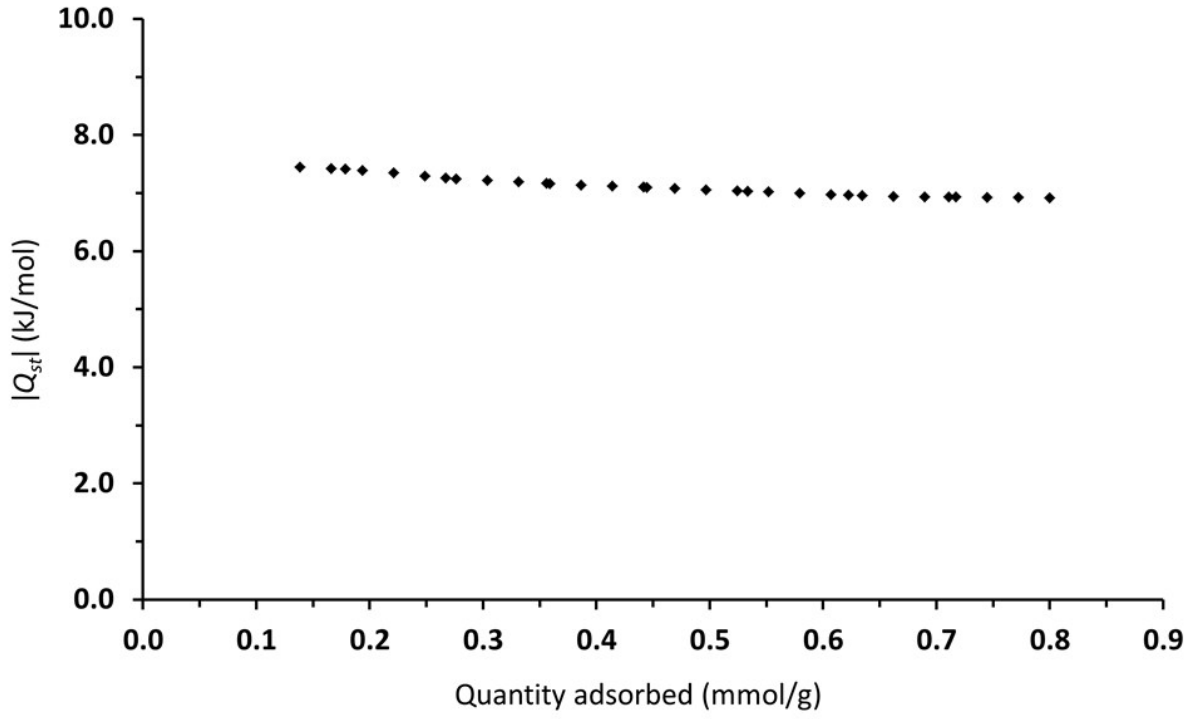

Figure S21. Zr-PzDC physisorption enthalpy as a function of H_2 loading.

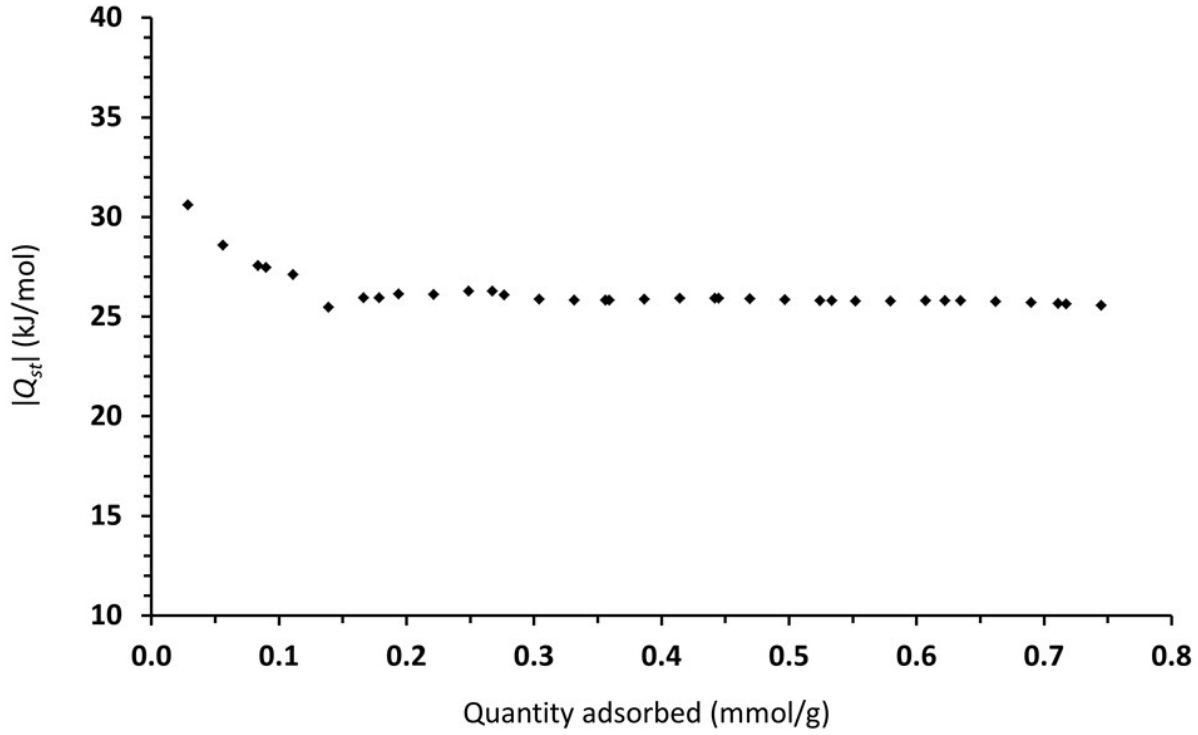

Figure S22. UiO-66 physisorption enthalpy as a function of CO_2 loading.

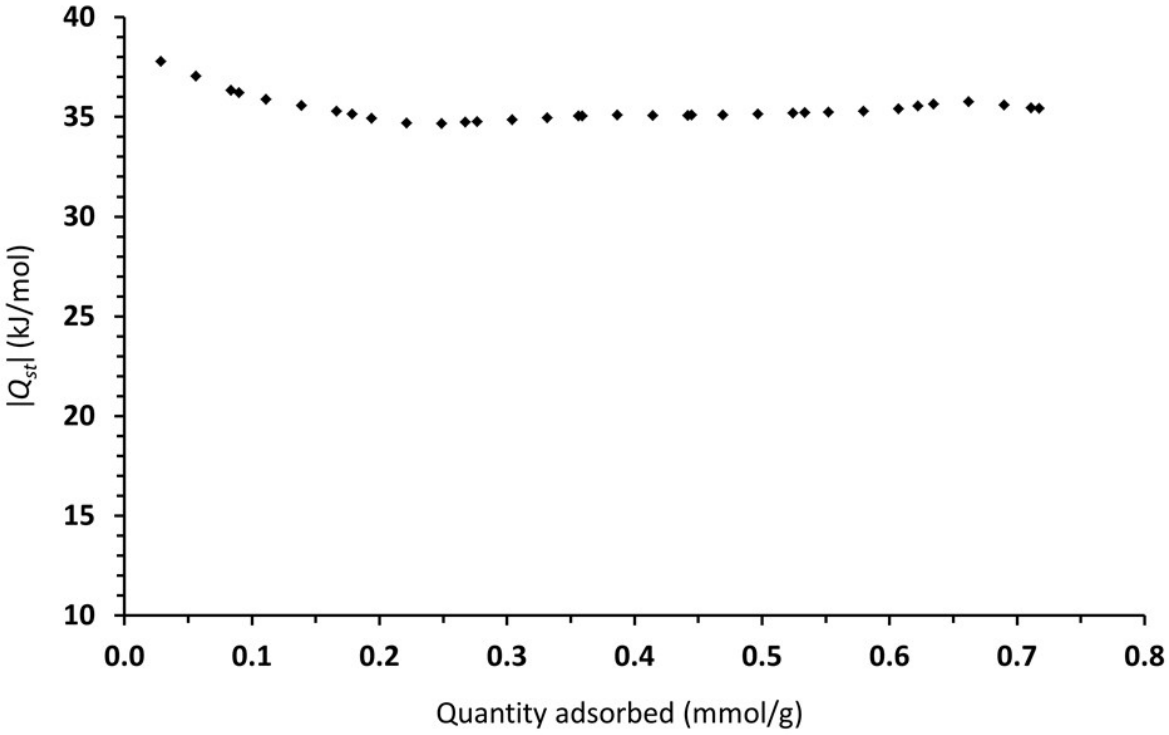

Figure S23. Zr-PyDC physisorption enthalpy as a function of CO_2 loading.

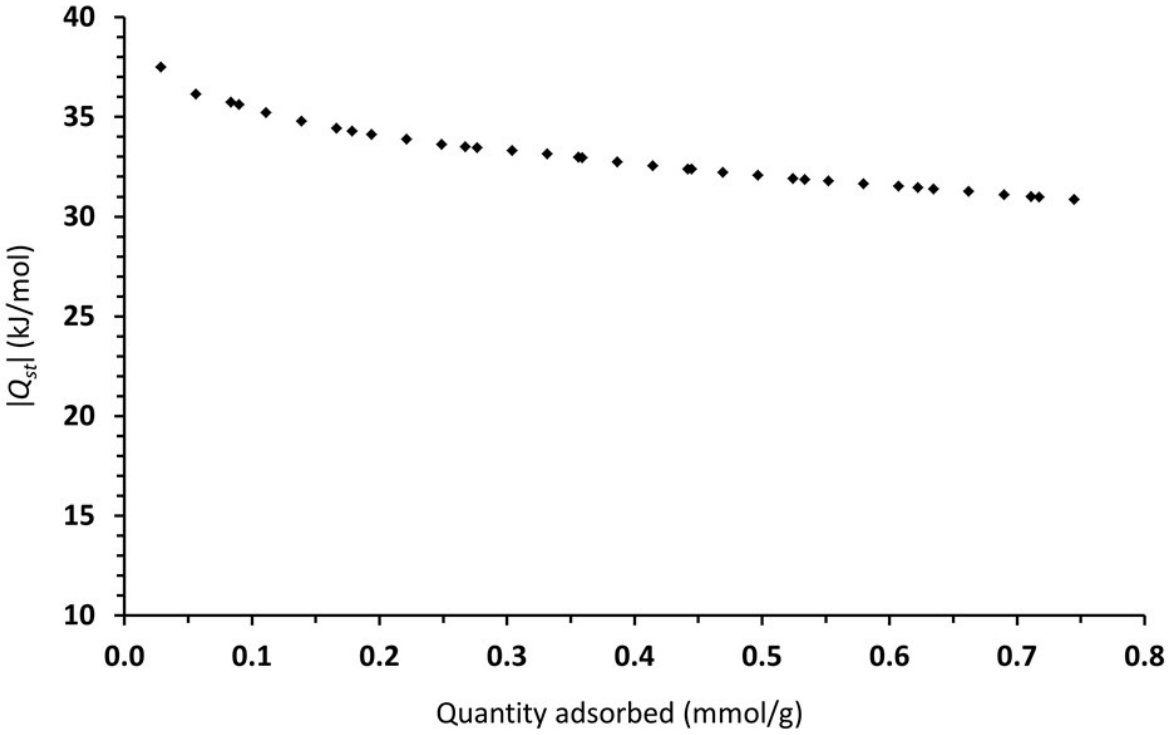

Figure S24. Zr-PyDC-MeI physisorption enthalpy as a function of CO_2 loading.

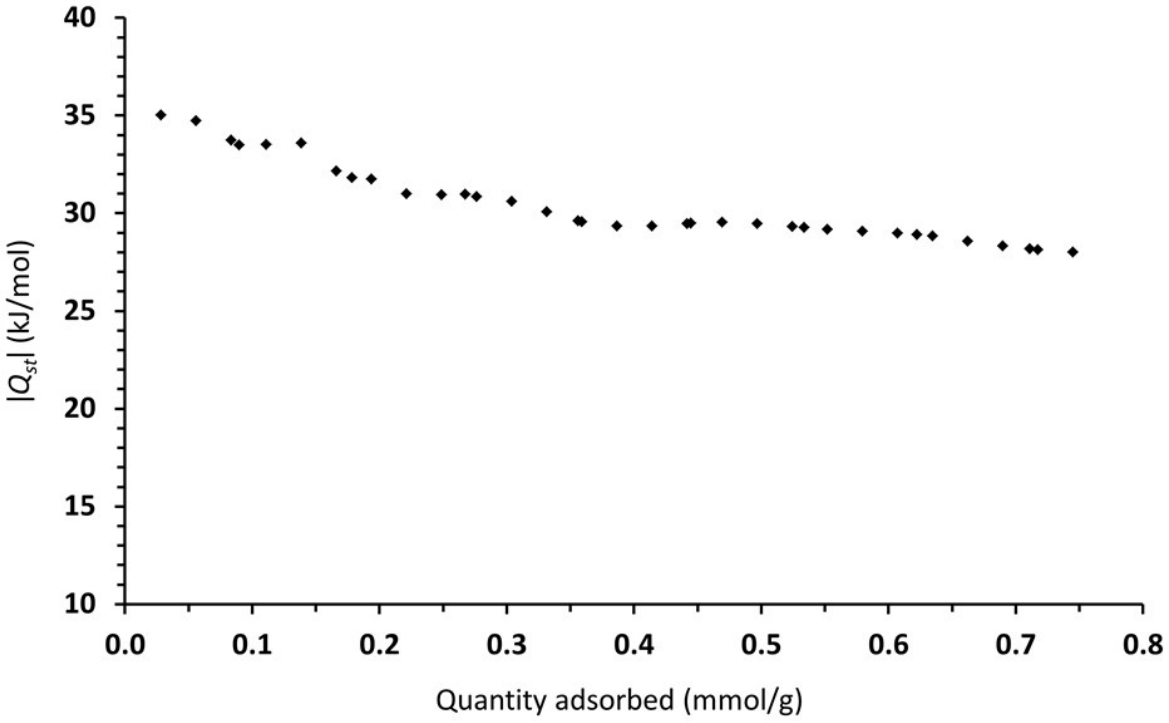

Figure S25. Zr-PyDC-Cu physisorption enthalpy as a function of CO_2 loading.

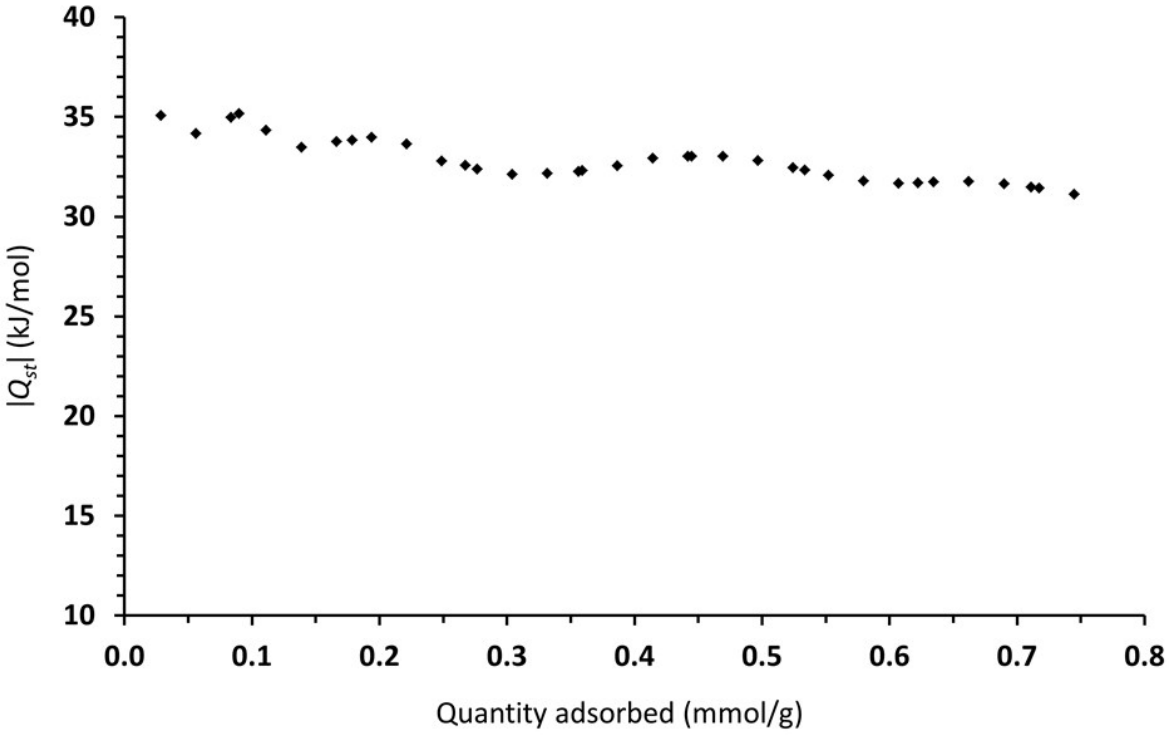

Figure S26. Zr-PzDC physisorption enthalpy as a function of CO_2 loading.

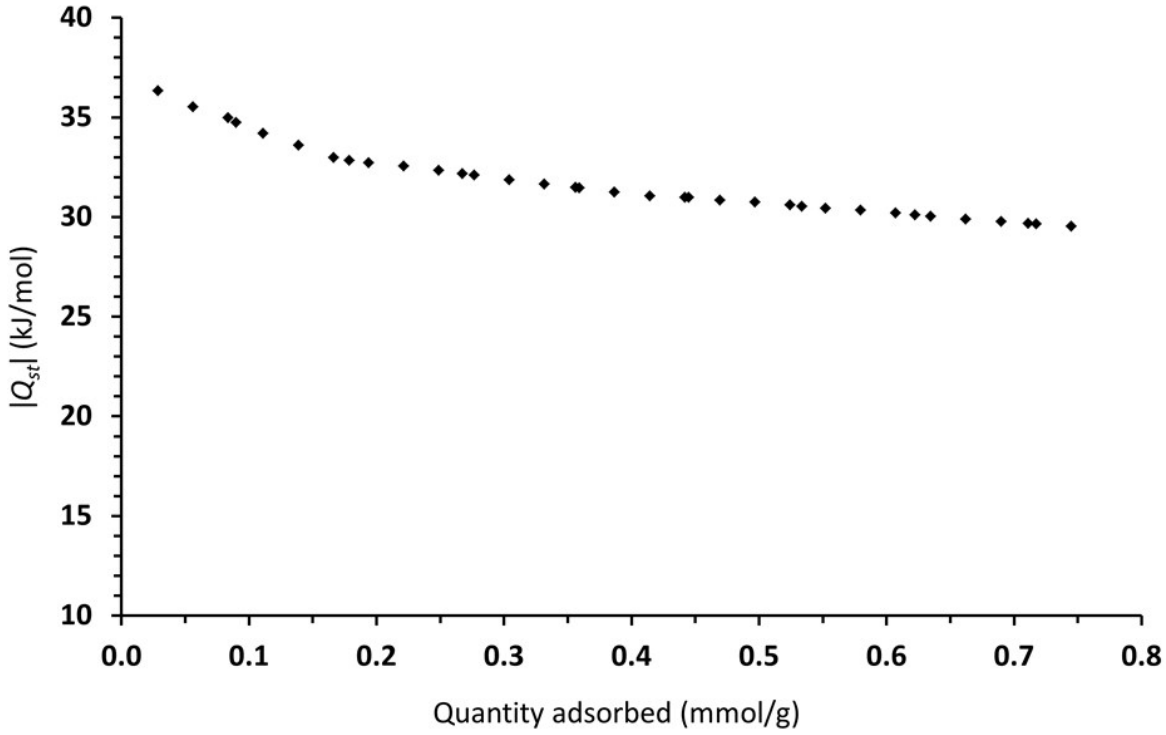

Figure S27. Zr-PzDC-MeI physisorption enthalpy as a function of CO_2 loading.

NLDFT.

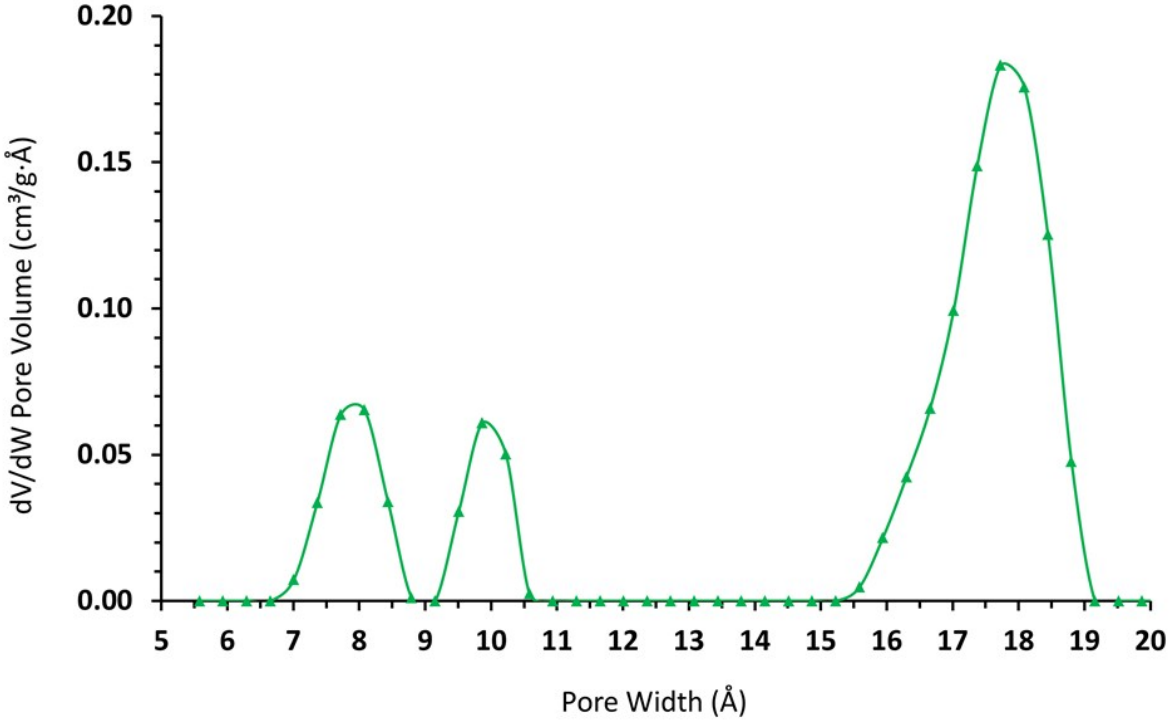

Figure S28. Zr-PyDC non-linear density function theory pore size distribution.

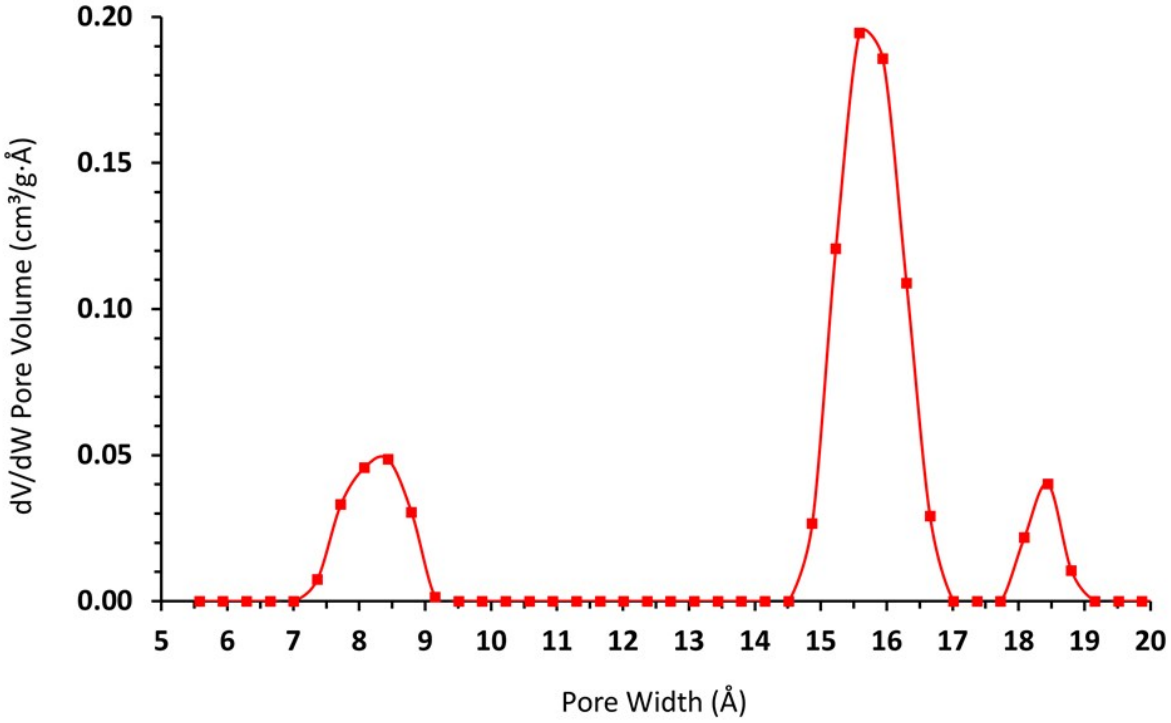

Figure S29. Zr-PyDC-MeI non-linear density function theory pore size distribution.

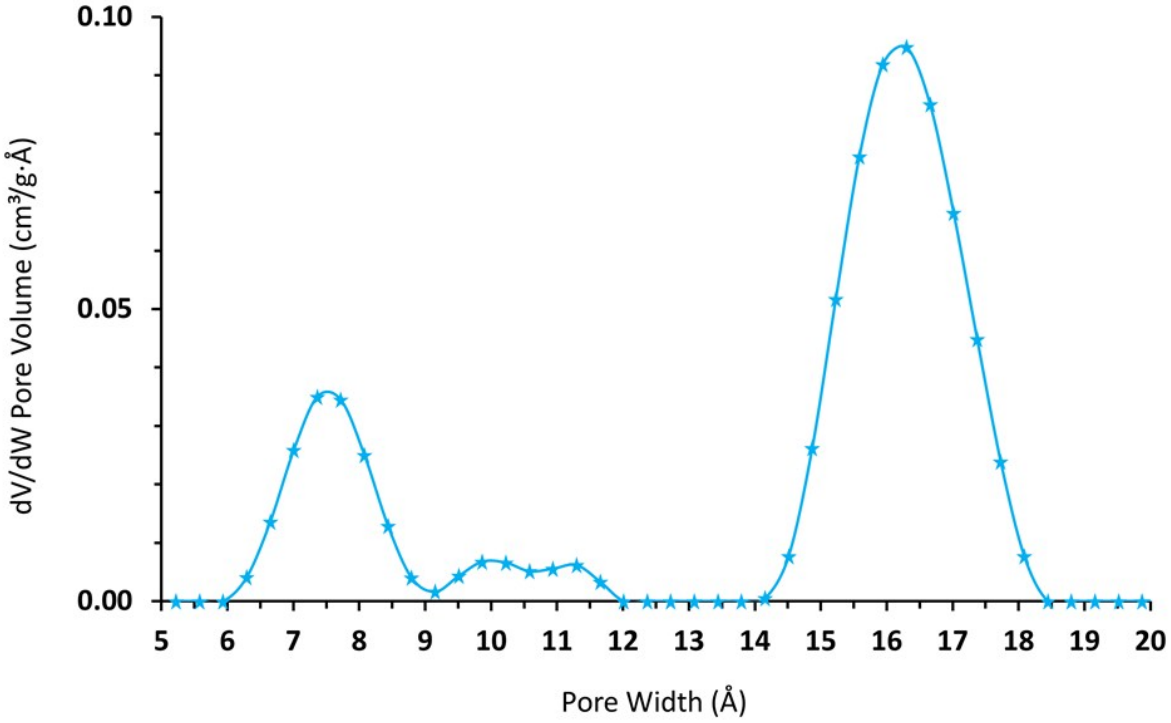

Figure S30. Zr-PyDC-Cu non-linear density function theory pore size distribution.

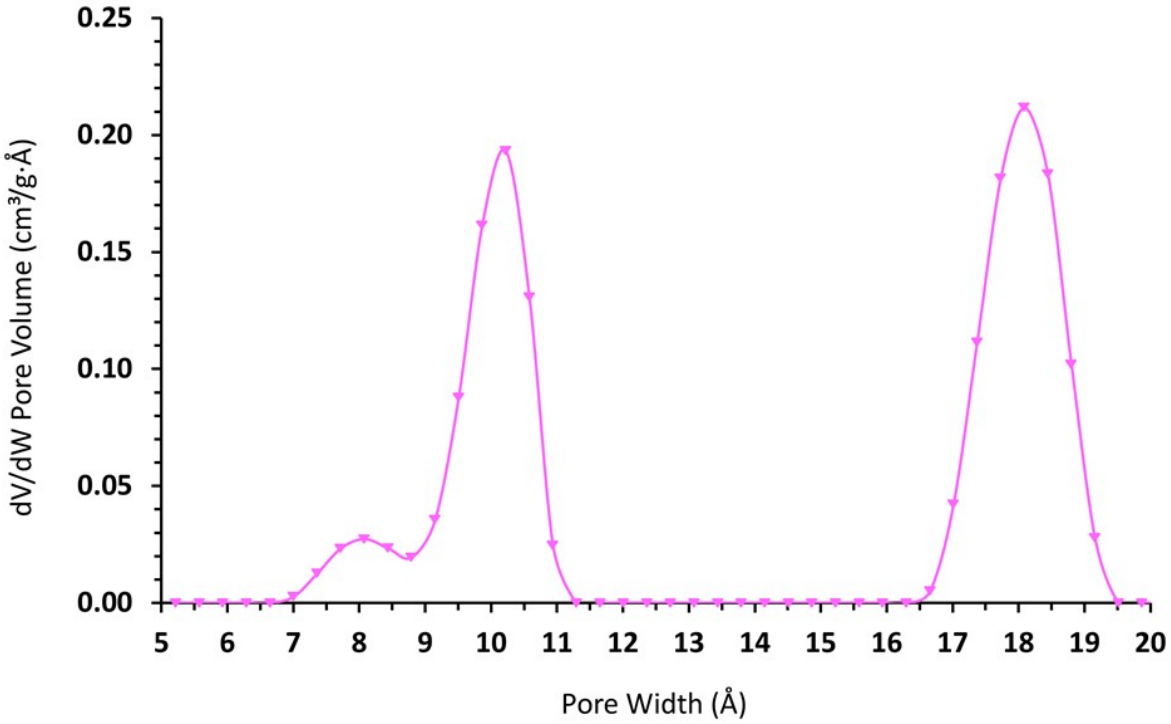

Figure S31. Zr-PzDC non-linear density function theory pore size distribution.

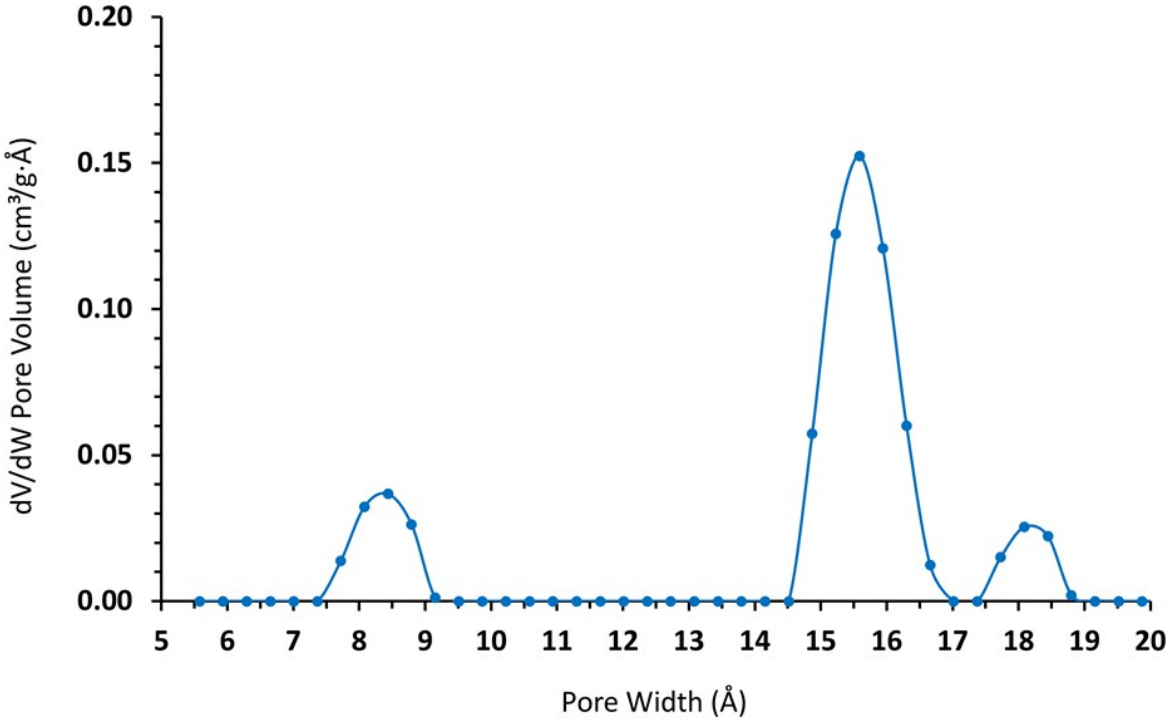

Figure S32. Zr-PzDC-MeI non-linear density function theory pore size distribution.

FTIR Spe

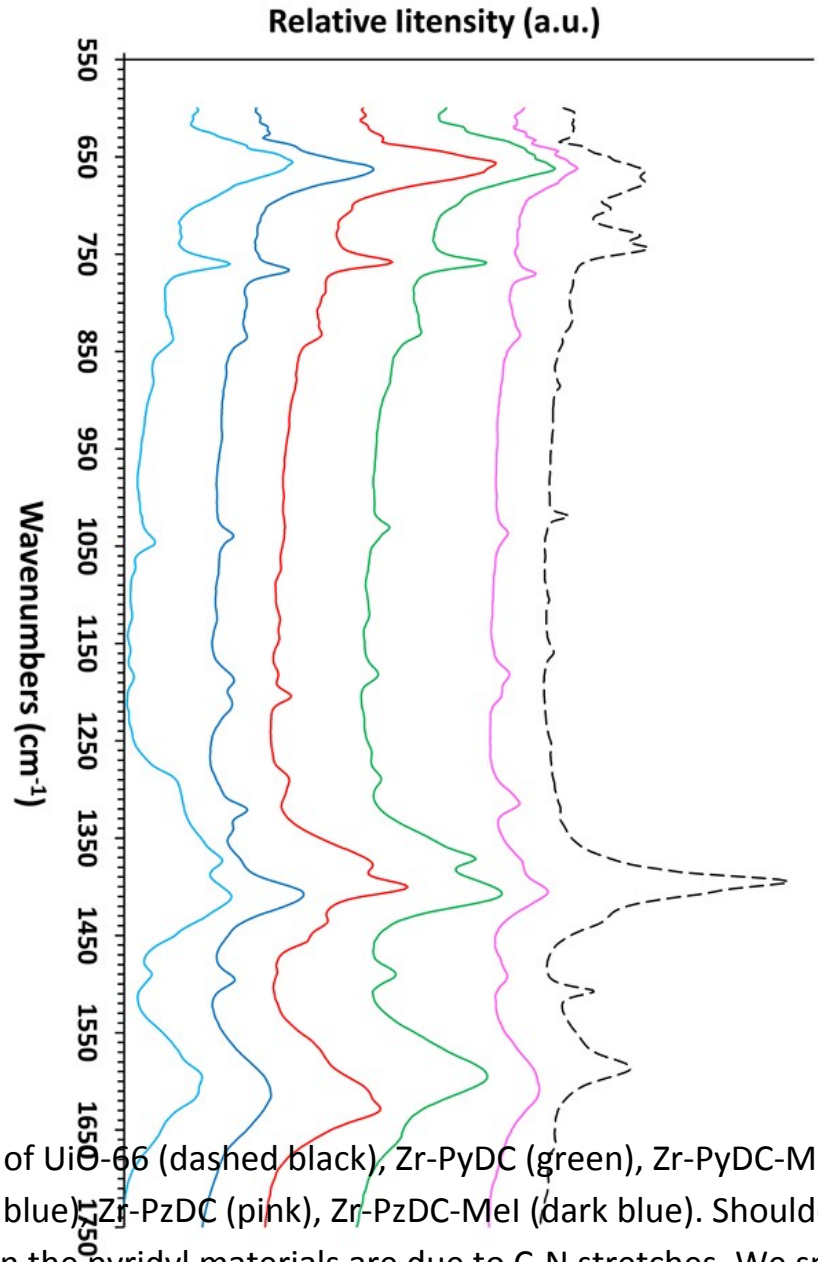

Figure S33. FTIR of UiO-66 (dashed black), Zr-PyDC (green), Zr-PyDC-MeI (red), Zr-PyDC-Cu (sky blue), Zr-PzDC (pink), Zr-PzDC-MeI (dark blue). Shoulders at circa 1300 cm^{-1} in the pyridyl materials are due to C-N stretches. We speculate that methyl C-H stretches in the methylated materials at circa 1450 cm^{-1} are obscured by the large carboxylate peak at circa 1390. We assign 600 – 850 cm^{-1} to C-H stretch.

Isosteric heat of adsorption

Isosteric heat of adsorption (Q_{st}) calculations for CO_2 and H_2 were performed using the Clausius–Clapeyron equation:

$$(lnP)_N = -\left(\frac{Q_{st}}{R}\right)\left(\frac{1}{T}\right) + C$$

where *P* is pressure, *N* is the amount adsorbed, *T* is temperature, *R* is the universal gas constant andarn *C* is a constant.